Genetic redundancy masks diverse functions of the tumor suppressor gene *PTEN* during *C. elegans* development

Yo Suzuki and Min Han[1]

Howard Hughes Medical Institute and Department of Molecular, Cellular, and Developmental Biology, University of Colorado, Boulder, Colorado 80309, USA

Genetic redundancy is associated with a large percentage of genes. We investigated *PTEN* (phosphatase and tensin homolog deleted on chromosome 10) tumor suppressor gene functions that eluded single mutant analyses, using a *Caenorhabditis elegans* genome-wide screen. We show that at least 27 genes collaborate with the worm *PTEN* homolog *daf-18* for various functions previously concealed by genetic redundancy, including embryogenesis, cuticle turnover, egg laying, and oocyte maturation. In one example, *daf-18* appears to constitute a cell-autonomous germline signal that converges with a somatic gonad signal mediated by *ceh-18* at a kinase inhibition. We provide evidence that *daf-18* elicits some functions independent of the downstream gene *daf-16*.

Supplemental material is available at http://genesdev.org.

Received September 23, 2005; revised version accepted December 22, 2005.

PTEN (phosphatase and tensin homolog deleted on chromosome 10) is a major tumor suppressor gene, controlling various processes such as cell cycle progression, cell survival, translation, and metabolism (Sulis and Parsons 2003). *PTEN* encodes a phosphatase that catalyzes the dephosphorylation of phophatydylinositol-3, 4, 5-trisphosphate (PIP_3), thereby antagonizing the role of phosphoinositide-3 (PI-3) kinase and Akt kinase/protein kinase B (Maehama and Dixon 1998; Sulis and Parsons 2003).

There is a single *PTEN* homolog (*daf-18*) in *Caenorhabditis elegans*. Loss-of-function (*lf*) mutations in *daf-18* block entry into the diapause (dauer) stage and reduce life span by affecting the *daf-2* (insulin receptor)/*age-1* (PI-3 kinase) pathway (Ogg and Ruvkun 1998). Unlike fly *dPTEN(lf)* mutants and mouse *PTEN(lf)* mutants, which are lethal as embryos (Sulis and Parsons 2003), the vast majority of *C. elegans daf-18(lf)* mutants complete normal development (Gil et al. 1999). We hypothesize that *daf-18* plays important roles in multiple aspects of *C. elegans* growth and development, yet many of the effects of *daf-18(lf)* mutations are masked by genetic redundancy mainly due to functions of genes that are not structurally related to *daf-18*. The viability of the *C. elegans* mutants should facilitate screening for genes that collaborate with *PTEN*. Previously, we and others have taken advantage of a similar characteristic for the *C. elegans Rb* gene (*lin-35*) (Lu and Horvitz 1998; Fay et al. 2002).

[*Keywords*: Synthetic screen; *daf-18*; *daf-16*; *ceh-18*; PI-3 kinase]
[1]Corresponding author.
E-MAIL mhan@colorado.edu; FAX (303) 735-0175.
Article and publication are at http://www.genesdev.org/cgi/doi/10.1101/gad.1378906.

Results and Discussion

daf-18 *is expressed in the germline*

We first examined the *daf-18* expression patterns using in situ hybridization. *daf-18* message was present predominantly in the germline in larvae and adults (93%, $n = 88$) (Supplementary Fig. S1). This is a specific signal not detected in the *daf-18* deletion mutant ($n = 89$) or in *glp-4(bn2)* animals ($n = 112$), where little germline proliferation occurs (Beanan and Strome 1992). The technique employed is not suitable for detecting *daf-18* expression in the embryos. A *daf-18* reporter gene was expressed in various cells including neurons in the nerve ring, gut cells, and embryonic cells (Masse et al. 2005; data not shown), although the prominent germline expression was not detected using this approach. These expression patterns suggest that *daf-18* has a role in the germline or embryos, in addition to the known role in dauer and life span regulation. Sterility (Ste) or embryonic lethality (Emb) may thus be a phenotype resulting from simultaneous inactivation of *daf-18* and a functionally redundant gene.

RNA interference (RNAi) screen reveals essential functions of daf-18 *in* C. elegans *development*

To identify genes that function redundantly with *daf-18*, we screened a *C. elegans* whole-genome RNAi library. RNAi is effective for knocking down genes in the germline and for uncovering maternal-effect phenotypes, and is therefore expected to be suitable for examining genes that function with *daf-18*. In this screen, we fed synchronized, starved L1 animals with *Escherichia coli* generating double-stranded RNA (dsRNA) for *C. elegans* genes (Materials and Methods). Among the 16,757 genes represented in the library, we found 27 genes that, when inactivated, cause a strong Ste or Emb phenotype in a *daf-18*-null mutant (Table 1). RNAi of two genes caused Emb, and RNAi of 25 genes caused Ste phenotypes in the *daf-18(lf)* mutant. Among the Ste genes, nine also caused a low level of Emb RNAi phenotypes, suggesting that these genes interact with *daf-18* in multiple stages of development.

In all cases tested, a *daf-18(rf)* (reduction-of-function) allele (Ogg and Ruvkun 1998) also had synthetic phenotypes (Table 1). In addition, another RNAi-sensitive strain *eri-1(lf)* (Kennedy et al. 2004) behaved similarly to the *daf-16(+); daf-18(+)* control strains. To confirm that the phenotypes we detected were the results of specific gene inactivation and not any deleterious effects of RNAi, we generated double mutants for several genes for which a mutation is available. *mec-8(lf)* mutations caused a maternal-effect, synthetic Emb phenotype (Table 2; see below), whereas *unc-73(rf)* and *goa-1(lf)* mu-

Table 1. *Genes that, when inactivated in a* daf-18*-null mutant, cause a strong synthetic phenotype*

Gene name (chromosome location)	Protein encoded	Brood size as an indication of sterility ± SD		
		daf18(+) [*eri-1*(*lf*)]	*daf-18*(*lf*) [*daf-18*(*rf*)]	*daf-16*(*lf*)
[Actin cytoskeleton]				
unc-73 (I)	Guanine nucleotide exchange factor	99 ± 16	5 ± 1	117 ± 4
sma-1 (V)	β_H-spectrin	143 ± 33	9 ± 1	143 ± 7
		[73 ± 10]	[2 ± 1]	
T25F10.6 (V)[a]	Calponin-like protein[a]	96 ± 19[a]	6 ± 4[a]	30 ± 18[a]
[Extracellular matrix]				
bli-5 (III)	Protease inhibitor	74 ± 19	4 ± 2	50 ± 4
		[56 ± 6]	[1 ± 1]	
col-98 (III)[a]	Cuticle collagen[a]	38 ± 8[a]	4 ± 1[a]	26 ± 11[a]
[G protein signaling]				
goa-1 (I)[a,b]	Heterotrimeric G protein α subunit Go[a]	76 ± 23[a]	2 ± 1[a]	19 ± 6[a]
str-30 (V)[a,b]	Sevem TM receptor[a]	94 ± 27[a]	6 ± 5[a]	38 ± 8[a]
srw-96 (V)[a,b]	Seven TM receptor[a]	115 ± 30[a]	6 ± 4[a]	26 ± 8[a]
[Transcription]				
egl-27 (II)[a,b]	MTA1 of the NuRD complex[a]	69 ± 8[a]	1 ± 1[a]	8 ± 3[a]
dpy-28 (III)[b]	Non-SMC condensin subunit	145 ± 24	6 ± 3	150 ± 16
ceh-18 (X)	POU homeodomain protein	94 ± 10	2 ± 2	125 ± 38
		[62 ± 18]	[1 ± 1]	
sex-1 (X)[b]	Nuclear hormone receptor	68 ± 10	1 ± 1	3 ± 1[a]
		[23 ± 9]	[0 ± 0]	
ttx-3 (X)[a]	LIM homeodomain protein[a]	156 ± 6[a]	4 ± 1[a]	38 ± 18[a]
D2021.1 (X)[a,b]	Protein with tetratricopeptide repeats and a jmjC domain[a]	34 ± 8[a]	2 ± 2[a]	11 ± 2[a]
		[48 ± 7]	[1 ± 1][a]	
[Others]				
hrp-1 (IV)	RNA/telomere-binding protein, splicing factor	109 ± 22	0 ± 0	99 ± 19
		[33 ± 36]	[0 ± 0]	
F25H2.5 (I)	NDP kinase	63 ± 8	3 ± 1	92 ± 17
nrf-6 (II)[a,b]	Acyltransferase[a]	64 ± 10[a]	4 ± 3[a]	15 ± 7[a]
		[90 ± 5]	[1 ± 1][a]	
vab-19 (II)[a]	Protein with ankyrin repeats[a]	87 ± 18[a]	2 ± 1[a]	26 ± 9[a]
		[88 ± 19]	[1 ± 1][a]	
Y48C3A.9 (II)[a]	Single-stranded DNA-binding protein with a lissencephaly type-1-like homology motif[a]	66 ± 14[a]	2 ± 1[a]	32 ± 5[a]
C53A3.2 (V)	Hydrolase	183 ± 3	16 ± 9	230 ± 32
F48G7.9 (V)[a]	Phorbol esters/diacylglycerol-binding domain protein[a]	115 ± 11[a]	3 ± 1[a]	67 ± 7[a]
Y113G7B.17 (V)[a]	Protein arginine N-methyltransferase[a]	33 ± 8[a]	1 ± 1[a]	26 ± 5[a]
		[27 ± 12]	[1 ± 1][a]	
F54D11.2 (V)[a,b]	Novel protein[a]	108 ± 6[a]	3 ± 2[a]	55 ± 2[a]
Y50D4B.7 (V)[a]	Novel protein[a]	129 ± 6[a]	6 ± 1[a]	51 ± 3[a]
		[115 ± 13]	[6 ± 4][a]	
Y51A2D.15 (V)[a]	Novel protein[a]	80 ± 11[a]	2 ± 1[a]	19 ± 7[a]
		[56 ± 53]	[0 ± 0][a]	
Vector	NA	128 ± 10	93 ± 5	201 ± 14
		[119 ± 20]	[45 ± 10]	
Vector[a]	NA[a]	75 ± 7[a]	31 ± 4[a]	58 ± 3[a]
			[35 ± 12][a]	

Gene name	Protein encoded	Embryonic lethal frequency (95% confidence interval)		
		daf-18(+)	*daf-18* (*lf*)	*daf-16* (*lf*)
mec-8 (I)	RNA-binding protein, splicing factor	8% (5–13%)	73% (62%–81%)	32% (27–38%)
dab-1 (II)	Adaptor protein, *Drosophila*-disabled homolog	8% (6–11%)	78% (69–85%)	93% (90–95%)
Vector	NA	4% (2–8%)	11% (8–15%)	0% (0–1%)

[a]Synthetic interaction was observed only in an *rrf-3*(*lf*) background. Data from the *rrf-3*(*lf*) strain is shown. For the other genes, synthetic interaction was observed in both *rrf-3*(*lf*) and non-*rrf-3*(*lf*) backgrounds, and data from the non-*rrf-3*(*lf*) strain is shown. (Highlighted) Data was statistically significant ($\alpha = 0.05$) compared with the *daf-16*(+); *daf-18*(+) control and with the vector control.
[b]RNAi also caused a low level of synthetic Emb phenotype in the *daf-18*(*lf*) mutant.

Table 2. *Interaction between* mec-8 *and* daf-18 *alleles*

Genotype of the parents	Emb% (*n*) 20°C
Wild type	2% (346)
mec-8 (*e398*)	1% (243)
daf-18 (*nr2037*)	1% (137)
mec-8; daf-18	94% (119)
mec-8+; daf-18	13% (1094)
mec-8; daf-18/+	7% (907)
mec-8; daf-18 × *mec-8* (males)	2% (174)
mec-8; daf-18 × *daf-18* (males)	5% (105)

tations caused a synthetic Ste phenotype with the *daf-18(lf)* mutation. The brood size of *unc-73(rf); daf-18(lf)* was 16 (10 parents examined), compared with 137 [*n* = 10, *unc-73(rf)*], 222 [*n* = 19, *daf-18(lf)*], or 261 (*n* = 10, wild type), and the brood size of *goa-1(lf); daf-18(lf)* was 8 (*n* = 11), compared with 45 [*n* = 9, *goa-1(lf)*]. Surprisingly, the brood size of *daf-18(lf); ceh-18(lf)* was 120 (*n* = 8), essentially identical to that of the single mutants [120, *n* = 8, *ceh-18(lf)*; see above]. However, when these animals were starved in the L1 stage as in the original screen, the brood sizes were 4 [*n* = 70, *daf-18(lf); ceh-18(lf)*], 70 [*n* = 10, *daf-18(lf)*], and 125 [*n* = 24, *ceh-18(lf)*]. Therefore, genetic mutations reproduced the RNAi data, validating that our RNAi approach was effective.

Identified genes interact with different branches of the daf-2 *pathway*

To examine whether the identified genes function with the *daf-2* pathway as a whole or with a branch including *daf-18*, we treated a *daf-16*-null mutant with RNAi of these genes. *daf-16* encodes a FOXO transcription factor, acting downstream of this pathway (Lin et al. 1997; Ogg et al. 1997). We found that for 14 Ste genes, the phenotypic enhancement between RNAi and the *daf-16(lf)* mutation was statistically insignificant ($\alpha = 0.05$) when compared with the effect of RNAi on the *daf-16(+)* control strain or with the phenotype of the untreated *daf-16(lf)* mutant (Table 1), consistent with the possibility that these genes interact with branches of the *daf-2* pathway that diverge upstream of *daf-16*. In agreement with these RNAi results, the Emb phenotype of the *mec-8(lf) daf-16(lf)* mutant was 83% penetrant (*n* = 308), comparable to that of the *mec-8(lf); daf-18(lf)* mutant, whereas the brood size of the *unc-73(lf) daf-16(lf)* mutant, unlike the *unc-73(lf); daf-18(lf)* mutant, was high (113, *n* = 10), similar to that of the *unc-73(lf)* single mutant (see above). The *daf-16(lf)* single mutant was 0.4% Emb (*n* = 500) and had the brood size of 199 (*n* = 9). In addition, *mec-8(lf); akt-1(gf)* (a gain-of-function mutation in a kinase gene that acts negatively on *daf-16*) was 34% Emb (*n* = 123), compared with 2% [*n* = 259; *akt-1(gf)*].

daf-18 *acts in parallel to* ceh-18 *in ovulation*

Among the 27 genes, four function with the actin cytoskeleton, three encode components in G-protein signal transduction pathways, two are related to the extracellular matrix, six affect transcription, and two encode splicing factors (Table 1). To investigate the synthetic phenotypes in detail, we focused on a few representative genes. *ceh-18* encodes a POU-class, homeodomain-containing transcription factor that regulates gonadal sheath cell differentiation (McCarter et al. 1997; Rose et al. 1997). *daf-18(lf); ceh-18*(RNAi) animals, when starved as L1s, had a Ste phenotype at a frequency of 77% (*n* = 44), compared with 10% [*n* = 40, *daf-18(lf)*], 0% [*n* = 38, *ceh-18*(RNAi)], 13% [*n* = 80, *ceh-18(lf)*], or 0% (*n* = 40, wild type). The gonads were often skinny and defective in migration in these animals, but these were defects also observed in the *daf-18(lf)* mutant not treated with RNAi. In addition, DAPI staining showed normal nuclear morphologies in the gonadal arm (data not shown).

Under Nomarski optics, we observed in all *daf-18(lf)* animals treated with *ceh-18* RNAi (*n* = 6), the first oocytes entered the spermatheca only halfway and clogged the ovary (Fig. 1A–C). The gonadal sheath contraction appeared to be too weak to complete ovulation. Later these gonads displayed a massively disorganized appearance probably due to the rupture or degradation of oocytes. Although the disorganized appearance was occasionally observed in the untreated *daf-18(lf)*, the rate of the first oocytes entering the spermatheca was high in the *daf-18(lf)* (five out of five) or *ceh-18(lf)* (three out of three) mutant.

In the wild-type germline, oocytes arrest at the diakinesis stage of meiotic prophase I prior to fertilization. Defective ovulation in *ceh-18(lf)* mutants deregulates this arrest, causing oocytes to undergo multiple rounds of DNA replication without cytokinesis to generate endomitotic (Emo) nuclei (Iwasaki et al. 1996; McCarter et al. 1997; Rose et al. 1997). Consistent with the enhancement interaction between *daf-18* and *ceh-18*, we found that the *daf-18(lf)* mutant treated with *ceh-18* RNAi had

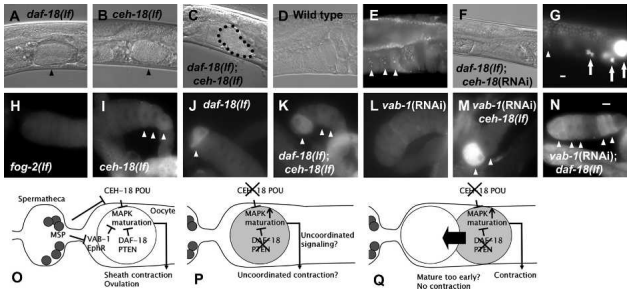

Figure 1. *daf-18* interacts with *ceh-18* to regulate oocyte maturation. (*A–C*) Ovulation of the first oocyte in indicated strains. These animals were starved as L1s. The oocyte entered the spermatheca (arrowheads) in *daf-18(lf)* and *ceh-18(lf)* mutants, but failed to complete ovulation in *daf-18(lf); ceh-18(lf)* (dotted line). (*D–G*) Nomarski (*D*,*F*) and DAPI staining (*E*,*G*) images showing the Emo phenotype (arrows) of oocyte nuclei. Arrowheads indicate normal diakinesis nuclei. (*H–N*) MAP kinase activation in oocytes of unmated females of indicated strains. These strains all contain *fog-2(lf)*. Stained oocytes are indicated with arrowheads in *I*, *J*, *K*, *M*, and *N*. (*O–Q*) Models to explain how *daf-18* and *ceh-18* pathways converge on MAP kinase to affect ovulation. (*O*) VAB-1 and CEH-18 constitute a mechanism that activates MAP kinase in response to sperm. Maturing oocytes send a signal to the sheath to stimulate contraction for ovulation. DAF-18 plays a cell-autonomous role in this mechanism by inhibiting MAP kinase in the oocyte through the PIP_3:PIP_2 ratio or AKT kinases, but not DAF-16. (*P*) When *daf-18* and *ceh-18* are inactivated, MAP kinase activity is deregulated in an additive manner. This may lead to uncoordinated signaling by the oocyte or to uncoordinated response by the sheath to the intense signal if animals are starved as L1s. (*Q*) Alternatively, the oocyte may mature too early in this condition for correct signaling. Bar, 0.01 mm (bar in *G* applies to *F*,*G*; bar in *N* applies to the rest).

a more penetrant Emo phenotype (84%, 50 gonads examined) than untreated *daf-18(lf)* (6%, *n* = 36) or *ceh-18*-null (19%, *n* = 79) (Fig. 1D–G).

daf-18 *functions in the germline for the interaction with* ceh-18

Since laser ablation of the gonadal sheath cells, where *ceh-18* functions, causes Emo at a higher frequency than a *ceh-18(lf)* mutation (McCarter et al. 1997; Rose et al. 1997), *daf-18* and *ceh-18* may function together in these cells. Alternatively, *daf-18* may function in the germline where it is expressed. To determine the site of action for *daf-18*, we treated *rrf-1(lf); ceh-18(lf)* animals with *daf-18* RNAi. The *rrf-1(lf)* mutation reduces the efficiency of RNAi in the soma (including the sheath cells), but not in the germline (Sijen et al. 2001). *daf-18* RNAi caused a Ste phenotype at a similar frequency in both the *ceh-18(lf)* mutant (72%, *n* = 32) and the *rrf-1(lf); ceh-18(lf)* mutant (73%, *n* = 22), suggesting that *daf-18* functions in the germline. The frequencies of Ste for the control strains were 0% [*n* = 20, *rrf-1(lf)*], 15% [*n* = 20, *rrf-1(lf); ceh-18(lf)*], 0% [*n* = 21, *daf-18*(RNAi)], and 5% [*n* = 20, *rrf-1(lf); daf-18*(RNAi)].

daf-18 *and* ceh-18 *control mitogen-activated protein (MAP) kinase activation in oocyte maturation*

ceh-18 constitutes part of the sperm-sensing mechanism dependent on the gonadal sheath cells that inhibits oocyte maturation (Miller et al. 2003). We tested the possibility that the molecular target of this mechanism, MAP kinase, is also controlled by *daf-18*. In the presence of sperm, MAP kinase activation, as assessed using an antibody directed against the phosphorylated form of MAP kinase, is observed in the two to three most proximal oocytes (Miller et al. 2001; Page et al. 2001; data not shown). To eliminate the influence of sperm, we examined unmated females resulting from a *fog-2(lf)* mutation (Schedl and Kimble 1988). As previously reported (Miller et al. 2003), MAP kinase activation in oocytes was detected in a *ceh-18(lf)* mutant (44% gonad stained, average 0.8 oocyte stained per gonad, *n* = 110), whereas it was rarely observed in the *fog-2(lf)* control (6%, 0.1, *n* = 133) (Fig. 1H–K; Supplementary Table 1). We found that a *daf-18(lf)* mutant also had activated MAP kinase (45%, 0.5, *n* = 119), suggesting that MAP kinase is the common target of *daf-18* and *ceh-18*. Consistent with the possibility that *daf-18* and *ceh-18* act in parallel, the percentage of gonads stained (60%) and the number of oocytes stained (1.3, *n* = 149) in a *daf-18(lf); ceh-18(lf)* double mutant were higher than in either single mutant. Starvation in the L1 stage did not further increase activated MAP kinase staining (51%, 0.9, *n* = 100), suggesting that the effect of starvation is mediated by a separate mechanism. It has been shown that the Eph receptor encoded by the *vab-1* gene functions as a receptor for major sperm protein (MSP) and also synergizes with *ceh-18* (Miller et al. 2003). We examined the relationship between *vab-1* and *daf-18* by inactivating *vab-1* in nonstarved larvae using RNAi (Fig. 1L–N). *vab-1* RNAi in *ceh-18(lf)* resulted in a dramatic increase in the intensity of staining (Fig. 1M); this was never observed with *vab-1* RNAi in the *daf-18(lf)* mutant, suggesting that *daf-18* and *ceh-18* function differently. These data are consistent with the possibility that *vab-1* and *daf-18* act in the same pathway. However, we noticed that multiple oocytes were stained at a higher frequency in *vab-1*(RNAi); *daf-18(lf)* (24%, *n* = 102) than in *daf-18(lf)* (5%, *n* = 119) or *vab-1*(RNAi) (2%, *n* = 83) (Supplementary Table 1), leaving open the possibility that *daf-18* constitutes a third pathway that modulates the activity of MAP kinase in the sperm-sensing mechanism. A signal from maturing oocyte has been known to stimulate the sheath contraction rate (McCarter et al. 1999). Based on these findings, we speculate that inactivation of *daf-18* and *ceh-18* results in misregulation of MAP kinase in oocytes that affects this signaling event and, together with an unknown developmental defect caused by L1 starvation, leads to sterility (Fig. 1O–Q).

The mec-8; daf-18 *double mutant has a maternal-effect Emb phenotype*

mec-8 is one of two genes that, when inactivated, caused F_1 Emb, but not P_0 Ste in the *daf-18(lf)* mutant. We found that Emb of the *mec-8(lf); daf-18(lf)* double mutant is a maternal-effect phenotype, observed only when parents are homozygous for both mutations (Table 2). Also, the Emb phenotype was rescued when a wild-type copy of *mec-8* or *daf-18* was introduced from sperm (paternally rescuable). These results suggest that the activities of *daf-18* and *mec-8* are provided both in the germline and in embryos, consistent with the expression patterns for *daf-18*. Previously *mec-8(lf)* mutants were shown to have a partially penetrant, cold-sensitive Emb phenotype (Lundquist and Herman 1994). The double mutant showed the same level of lethality at all temperatures tested (Supplementary Table 2). The *mec-1(lf); daf-18(lf)* double mutant did not have significant lethality (2% Emb, *n* = 260), indicating that not all *mec* (mechanosensory-defective; WormBase) genes interact with *daf-18*.

daf-18 *functions with* mec-8 *in embryonic elongation*

mec-8 (RNA-binding protein) controls the alternative splicing of *unc-52*, which encodes the integrin ligand perlecan (Rogalski et al. 1993; Lundquist et al. 1996; Spike et al. 2002). Among the arrested *mec-8*(RNAi); *daf-18(lf)* embryos (*n* = 100), 72% arrested around the two-fold stage similar to integrin pathway mutants (Rogalski et al. 1993; Williams and Waterston 1994), and the rest (28%) assumed an exploded appearance similar to *gex* (gut on the exterior) mutants that are related to Rac GTPase functions (Fig. 2A–C). These embryos also had a lumpy appearance reminiscent of the phenotype of *hmp* (humpback) mutants that are related to the cadherin complex (Piekny and Mains 2003). Therefore, *mec-8*(RNAi); *daf-18(lf)* embryos have aspects of multiple elongation-defective phenotypes, possibly reflecting the sharing of components or the existence of cross-talk among different pathways. Consistent with the idea that the primary defect for lethality lies in the integrin pathway, the *mec-8*(RNAi); *daf-18(lf)* embryos had a defect in muscle organization as in integrin pathway mutants (Fig. 2D–F), and the frequency of this defect (55%, *n* = 20) was comparable to that of Emb (63%, *n* = 214) in these experiments. We carried out additional experiments to identify potential targets of this interaction without success (Supplemental Material).

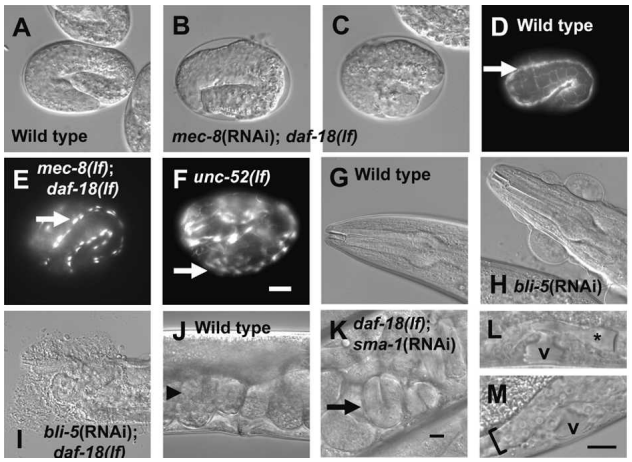

Figure 2. (*A–F*) The *mec-8(lf); daf-18(lf)* embryos arrest in the twofold stage. (*A*) Wild-type embryo reaching the threefold stage. (*B*) *mec-8*(RNAi); *daf-18(lf)* embryo that has arrested at the twofold stage. (*C*) *mec-8*(RNAi); *daf-18(lf)* embryo that has exploded (all examined 500 min after the first cleavage at 25°C). (*D–F*) Myosin heavy chain A antibody staining showing muscle organization. Muscles (arrows) formed continuous bundles in wild type, but were fragmented in *mec-8(lf); daf-18(lf)* and *unc-52(lf)*. The MH27 antibody that stains the apical junctions of epidermal cells (grid-like patterns) was included as a temporal marker. (*G–I*) *daf-18* interacts with *bli-5*. The head regions of indicated strains are shown. (*J–M*) *daf-18* interacts with *sma-1*. (*J*) Egg lining in wild type. Arrowhead points to a normal egg. (*K*) Egl phenotype of *daf-18(lf); sma-1*(RNAi). Arrow indicates a late-stage embryo. (*L,M*) Developing uteri in L4-stage larvae. The uterine lumen (asterisk) is adjacent to the vulva (v) in *daf-18(lf)* (*L*), but is not found in a corresponding region (bracket) in *daf-18(lf); sma-1*(RNAi) (*M*). Bar, 0.01 mm (bar in *F* applies to *A–F*; bar in *K* applies to *G–K*; bar in *M* applies to *L,M*).

daf-18 *interacts with* bli-5 *to regulate cuticle turnover*

bli-5 encodes a protease inhibitor required for the integrity of the adult cuticle (WormBase). When *daf-18(lf)* mutants were treated with *bli-5* RNAi, a striking phenotype was observed where animals exploded from the head region (60%, $n = 64$ vs. 0% in untreated animals, $n > 100$) (Fig. 2G–I). *bli-5* RNAi caused the blister (Bli) phenotype, where fluid accumulates between the cuticle and the epidermal cells (Fig. 2H), but only rarely caused explosion in wild type (0%, $n = 39$) or *rrf-3(lf)* (3%, $n = 74$). Therefore, the *daf-18(lf)* mutation enhances the cuticle defects of the *bli-5* RNAi-treated animals. *daf-18* may act upstream of genes encoding the matrix proteases targeted by BLI-5 or on the hormonal control of molting.

daf-18 *and* sma-1 *are required for egg laying*

sma-1 encodes a β_H-spectrin required for embryonic elongation (McKeown et al. 1998). RNAi of *sma-1* on the *daf-18(lf)* strain caused an egg-laying-defective (Egl) phenotype (38%, $n = 198$) (Fig. 2J,K). This phenotype was infrequent in wild type treated with *sma-1* RNAi (3%, $n = 149$), the *rrf-3(lf)* mutant treated with *sma-1* RNAi (13%, $n = 165$), or a *sma-1*-null mutant (13%, $n = 197$). Therefore, the weak Egl phenotype caused by *sma-1* inactivation is enhanced by the *daf-18(lf)* mutation. We found that the developing uterus was grossly abnormal in the L4 stage. In wild type, the uterine lumen and vulval invagination are separated by a thin membrane (Fig. 2L; Newman et al. 1996). In the *daf-18(lf)* mutant treated with *sma-1* RNAi, the uterine lumen was sometimes fragmented (35%, $n = 20$) or nonexistent (10%) (Fig. 3M). In other cases, the lumen contained cells that appeared to be undergoing necrosis (40%). Overall, 84% ($n = 22$) of the L4 stage vulva was not adjacent to the uterine opening, probably resulting in the accumulation of fertilized eggs in the uterus and the low brood size.

Concluding remarks

The processes protected by genetic redundancy are likely to be important to the cell and demand rigorous investigation. We show that the requirement for the *PTEN* homolog in animal survival and propagation is no different in *C. elegans*. The genetic redundancy we see in *C. elegans* for the developmental function of *PTEN* is also unlikely to be unique. For example, *PTEN* is expressed in mammalian skeletal muscles, where the PI-3 kinase pathway controls cell growth and differentiation, as well as glucose metabolism. However, the tissue-specific inactivation of *PTEN* in skeletal muscles does not result in any discernible phenotypes (Crackower et al. 2002). Some of the diverse functions we found in *C. elegans* for *daf-18* are related to cell cycle regulation, extracellular matrix turnover, and assembly of the actin cytoskeleton. These are fundamental processes in development and are possibly related to *PTEN* functions in mammals.

We found that inactivation of *daf-18* and *ceh-18* results in MAP kinase activation in maturing oocytes. Interestingly, the PI-3 kinase pathway is also involved in oocyte maturation in mouse (Hoshino et al. 2004). Somatic gonadal sheath cells may be considered analogous to the mammalian follicle cells, which also inhibit oocyte maturation. Therefore, it is possible that the mechanisms of synthetic interactions involving *PTEN* are conserved at the molecular level, underscoring the significance of our findings in the *C. elegans* system.

Materials and methods

C. elegans *strains*

Information regarding the mutants used in this study is found in WormBase (http://www.wormbase.org). The detail is described in the Supplemental Material.

In situ hybridization

Starved L1 animals were grown for ~48 h at 25°C, the restrictive temperature for *glp-4(bn2ts)* (Beanan and Strome 1992), and were fixed and stained (Mochii et al. 1999). The probe was generated using sequences deleted in the *nr2037* mutation (Gil et al. 1999).

Starvation

Starved, synchronized L1s, free of contaminating bacteria, were used to obtain consistent RNAi results, except in *vab-1* experiments where fed L1s were used and *rrf-1* experiments where progeny of animals starved as L1s were analyzed. To obtain starved L1 animals, eggs released from gravid hermaphrodites using a standard bleach treatment were cultured for 24 h at 16°C for the screen and for 18 h at 20°C for all the other tests. Starved *daf-18(lf)* L1s without bleach treatment were also Ste when treated with *ceh-18* RNAi.

RNAi screen

RNAi screen was performed using a feeding library (Kamath et al. 2003). The detail for the screen process is described in the Supplemental Material.

Real-time quantitative PCR (qPCR)

Young gravid hermaphrodites were bleached to release embryos, which were harvested when the midpoint of development reached the embry-

onic 1.5-fold stage. Standard protocols were used for RNA extraction, cDNA synthesis (poly-A-primed), and qPCR.

Microscopy

Embryos were fixed and stained using a hypochlorite method (Rogalski et al. 1993). Gonads were dissected out and stained as described (Miller et al. 2001). See Supplemental Material for details.

Acknowledgments

We thank C. Johnson for the *daf-18(nr2037)* allele; M. Fukuyama and J. Rothman for communicating unpublished results; J. Ahringer for the RNAi library; W. Wood, D. Fay, J. Schwarzbauer, K. Hirono, M. Ohmachi, R. Herman, M. Cui, J. Blanchette, M. Tucker, and D. Killian for advice; and CGC for strains. This project was funded by the HHMI, of which Y.S. was an associate and M.H. is an investigator.

References

Beanan, M.J. and Strome, S. 1992. Characterization of a germ-line proliferation mutation in *C. elegans*. *Development* **116:** 755–766.

Crackower, M.A., Oudit, G.Y., Kozieradzki, I., Sarao, R., Sun, H., Sasaki, T., Hirsch, E., Suzuki, A., Shioi, T., Irie-Sasaki, J., et al. 2002. Regulation of myocardial contractility and cell size by distinct PI3K–PTEN signaling pathways. *Cell* **110:** 737–749.

Fay, D.S., Keenan, S., and Han, M. 2002. fzr-1 and lin-35/Rb function redundantly to control cell proliferation in *C. elegans* as revealed by a nonbiased synthetic screen. *Genes & Dev.* **16:** 503–517.

Gil, E.B., Malone Link, E., Liu, L.X., Johnson, C.D., and Lees, J.A. 1999. Regulation of the insulin-like developmental pathway of *Caenorhabditis elegans* by a homolog of the *PTEN* tumor suppressor gene. *Proc. Natl. Acad. Sci.* **96:** 2925–2930.

Hoshino, Y., Yokoo, M., Yoshida, N., Sasada, H., Matsumoto, H., and Sato, E. 2004. Phosphatidylinositol 3-kinase and Akt participate in the FSH-induced meiotic maturation of mouse oocytes. *Mol. Reprod. Dev.* **69:** 77–86.

Iwasaki, K., McCarter, J., Francis, R., and Schedl, T. 1996. *emo-1*, a *Caenorhabditis elegans* Sec61p γ homologue, is required for oocyte development and ovulation. *J. Cell Biol.* **134:** 699–714.

Kamath, R.S., Fraser, A.G., Dong, Y., Poulin, G., Durbin, R., Gotta, M., Kanapin, A., Le Bot, N., Moreno, S., Sohrmann, M., et al. 2003. Systematic functional analysis of the *Caenorhabditis elegans* genome using RNAi. *Nature* **421:** 231–237.

Kennedy, S., Wang, D., and Ruvkun, G. 2004. A conserved siRNA-degrading RNase negatively regulates RNA interference in *C. elegans*. *Nature* **427:** 645–649.

Lin, K., Dorman, J.B., Rodan, A., and Kenyon, C. 1997. *daf-16*: An HNF-3/forkhead family member that can function to double the life-span of *Caenorhabditis elegans*. *Science* **278:** 1319–1322.

Lu, X. and Horvitz, H.R. 1998. *lin-35* and *lin-53*, two genes that antagonize a *C. elegans Ras* pathway, encode proteins similar to Rb and its binding protein RbAp48. *Cell* **95:** 981–991.

Lundquist, E.A. and Herman, R.K. 1994. The *mec-8* gene of *Caenorhabditis elegans* affects muscle and sensory neuron function and interacts with three other genes: *unc-52*, *smu-1* and *smu-2*. *Genetics* **138:** 83–101.

Lundquist, E.A., Herman, R.K., Rogalski, T.M., Mullen, G.P., Moerman, D.G., and Shaw, J.E. 1996. The *mec-8* gene of *C. elegans* encodes a protein with two RNA recognition motifs and regulates alternative splicing of unc-52 transcripts. *Development* **122:** 1601–1610.

Maehama, T. and Dixon, J.E. 1998. The tumor suppressor, PTEN/MMAC1, dephosphorylates the lipid second messenger, phosphatidylinositol 3,4,5-trisphosphate. *J. Biol. Chem.* **273:** 13375–13378.

Masse, I., Molin, L., Billaud, M., and Solari, F. 2005. Lifespan and dauer regulation by tissue-specific activities of *Caenorhabditis elegans* DAF-18. *Dev. Biol.* **286:** 91–101.

McCarter, J., Bartlett, B., Dang, T., and Schedl, T. 1997. Soma–germ cell interactions in *Caenorhabditis elegans*: Multiple events of hermaphrodite germline development require the somatic sheath and spermathecal lineages. *Dev. Biol.* **181:** 121–143.

———. 1999. On the control of oocyte meiotic maturation and ovulation in *Caenorhabditis elegans*. *Dev. Biol.* **205:** 111–128.

McKeown, C., Praitis, V., and Austin, J. 1998. *sma-1* encodes a βH-spectrin homolog required for *Caenorhabditis elegans* morphogenesis. *Development* **125:** 2087–2098.

Miller, M.A., Nguyen, V.Q., Lee, M.H., Kosinski, M., Schedl, T., Caprioli, R.M., and Greenstein, D. 2001. A sperm cytoskeletal protein that signals oocyte meiotic maturation and ovulation. *Science* **291:** 2144–2147.

Miller, M.A., Ruest, P.J., Kosinski, M., Hanks, S.K., and Greenstein, D. 2003. An Eph receptor sperm-sensing control mechanism for oocyte meiotic maturation in *Caenorhabditis elegans*. *Genes & Dev.* **17:** 187–200.

Mochii, M., Yoshida, S., Morita, K., Kohara, Y., and Ueno, N. 1999. Identification of transforming growth factor-β-regulated genes in *Caenorhabditis elegans* by differential hybridization of arrayed cDNAs. *Proc. Natl. Acad. Sci.* **96:** 15020–15025.

Newman, A.P., White, J.G., and Sternberg, P.W. 1996. Morphogenesis of the *C. elegans* hermaphrodite uterus. *Development* **122:** 3617–3626.

Ogg, S. and Ruvkun, G. 1998. The *C. elegans* PTEN homolog, DAF-18, acts in the insulin receptor-like metabolic signaling pathway. *Mol. Cell* **2:** 887–893.

Ogg, S., Paradis, S., Gottlieb, S., Patterson, G.I., Lee, L., Tissenbaum, H.A., and Ruvkun, G. 1997. The Fork head transcription factor DAF-16 transduces insulin-like metabolic and longevity signals in *C. elegans*. *Nature* **389:** 994–999.

Page, B.D., Guedes, S., Waring, D., and Priess, J.R. 2001. The *C. elegans* E2F- and DP-related proteins are required for embryonic asymmetry and negatively regulate Ras/MAPK signaling. *Mol. Cell* **7:** 451–460.

Piekny, A.J. and Mains, P.E. 2003. Squeezing an egg into a worm: *C. elegans* embryonic morphogenesis. *Scientific World Journal* **3:** 1370–1381.

Rogalski, T.M., Williams, B.D., Mullen, G.P., and Moerman, D.G. 1993. Products of the *unc-52* gene in *Caenorhabditis elegans* are homologous to the core protein of the mammalian basement membrane heparan sulfate proteoglycan. *Genes & Dev.* **7:** 1471–1484.

Rose, K.L., Winfrey, V.P., Hoffman, L.H., Hall, D.H., Furuta, T., and Greenstein, D. 1997. The POU gene *ceh-18* promotes gonadal sheath cell differentiation and function required for meiotic maturation and ovulation in *Caenorhabditis elegans*. *Dev. Biol.* **192:** 59–77.

Schedl, T. and Kimble, J. 1988. *fog-2*, a germ-line-specific sex determination gene required for hermaphrodite spermatogenesis in *Caenorhabditis elegans*. *Genetics* **119:** 43–61.

Sijen, T., Fleenor, J., Simmer, F., Thijssen, K.L., Parrish, S., Timmons, L., Plasterk, R.H., and Fire, A. 2001. On the role of RNA amplification in dsRNA-triggered gene silencing. *Cell* **107:** 465–476.

Spike, C.A., Davies, A.G., Shaw, J.E., and Herman, R.K. 2002. MEC-8 regulates alternative splicing of *unc-52* transcripts in *C. elegans* hypodermal cells. *Development* **129:** 4999–5008.

Sulis, M.L. and Parsons, R. 2003. PTEN: From pathology to biology. *Trends Cell. Biol.* **13:** 478–483.

Williams, B.D. and Waterston, R.H. 1994. Genes critical for muscle development and function in *Caenorhabditis elegans* identified through lethal mutations. *J. Cell Biol.* **124:** 475–490.